Chemical Physics 528 (2020) 110532

Contents lists available at ScienceDirect

Chemical Physics

journal homepage: www.elsevier.com/locate/chemphys

Volt-ampere characteristics of porcine retinal Müller cell intermediate filaments

Vladimir Makarov[a,*], Igor Khmelinskii[b]

[a] University of Puerto Rico, Rio Piedras Campus, PO Box 23343, San Juan, PR 00931-3343, USA
[b] Universidade do Algarve, FCT, DQB and CEOT, 8005-139 Faro, Portugal

ARTICLE INFO

Keywords:
Porcine retina
Müller cell
Intermediate filament
Light energy transmission
Light energy guide

ABSTRACT

In the current study we reported current-voltage (*I/V*) characteristics of Müller cell (MC) intermediate filaments (IFs) isolated from porcine retina. It was found that the measured *I/V* dependences demonstrate behavior of a semiconductor in contact with metal (Au) electrodes. The analysis of the temperature dependence of the experimental *I/V* curves produced estimates of the parameter values characterizing the electrical conductivity properties of the studied MC IFs. The *I/V* characteristics and the parameter values allowed to describe the MC IFs as a semiconducting material. The observed properties clarify the mechanism of high-contrast daylight vision of vertebrate eyes. This mechanism was extensively discussed earlier, and is directly dependent on the electric conductivity properties of MC IFs.

Significance Statement: Retinal cones and rods are physically connected to glial Müller cells by intermediate filaments (IFs). Electric conductivity of IFs allows for a simple quantum mechanical description of light energy transmission through the retina, providing a convincing mechanism that achieves high-contrast vision in vertebrate eyes. Note that classic light transmission is hindered by light scattering on the retinal structures. Electric conductivity of IFs also opens the possibility for energy exchange within and between other cell types by way of IFs and microtubules, and the possibility that such structures may be used for signaling e.g. in the nervous system.

1. Introduction

Recently a significant body of work has been devoted to understanding of the high-contrast vision of the vertebrate eye [1–9]. Among other ideas, mechanism of light focusing by the intracell organelles in the photoreceptor cells was proposed [1,2]. Another classical mechanism extensively discussed earlier [3–9] considers glial Müller cells (MCs) as natural light guides. However, it is still unclear how the light could pass through an inverted retina of vertebrates without significant scattering, and create high-contrast visual perception. Indeed, light scattering on subcellular structures remained a problem in all of the previously proposed models [1–9].

It has been proposed earlier that intermediate filaments (IFs) in the vertebrate retinal MCs have an additional function of the light energy guide, and transfer photon energy from the inner limiting membrane (ILM) level to the retinal photoreceptors [10–14]. To explain the IF properties, quantum mechanism of light energy transfer has been proposed [12,15]. This mechanism predicts that the extremities of the IFs located in the apex of the MC conical endfoot absorb photons and generate excitons. These excitons propagate along the IFs, and arrive to rhodopsin/opsin molecules of the photoreceptor cells [12,15]. The exciton transfer to the respective rhodopsin/opsin molecules should occur by the energy exchange contact mechanism [15]. The proposed quantum mechanical description of the energy transfer benefited from the postulated electrical conductivity of the MC IFs [12,15], which allowed to solve the respective energy transfer models analytically. Indeed, it was found earlier [16,17] that porcine retinal MC IFs have very low electrical resistance, which is comparable to that of metals. However, the measurements reported earlier [16,17] were carried out at a single bias voltage of 1.0 V. Therefore, the available results do not allow discriminating electric conductor IFs from semiconductor IFs. This is a very important issue for further development of the mechanism of light energy propagation through an inverted retina without scattering.

Previously we already reported that the potential difference applied to MC IFs isolated from porcine retina affects the efficiency of light energy transfer along these IFs [18]. Our present goal is to understand whether the energy transfer efficiency may be modulated by a periodic potential difference applied to the IFs. The existence of modulation

* Corresponding author.
E-mail address: vladimir.makarov@upr.edu (V. Makarov).

https://doi.org/10.1016/j.chemphys.2019.110532
Received 20 December 2018; Received in revised form 11 August 2019; Accepted 11 September 2019
Available online 12 September 2019
0301-0104/ Published by Elsevier B.V.

would enable the brain to separate the high-contrast image generated by the quantum mechanism (QM) from the low-contrast image generated by classical mechanisms. Such modulation might be possible as the MC membrane has an electric potential of ca. 100 mV, and the MC IFs interact with the membrane. It is unclear whether the MC membrane potential is in fact periodically variable; therefore, we hope that the respective measurements will be stimulated by our recent results [18]. Note that the *I/V* characteristics recorded at constant temperature demonstrated semiconducting properties of the IFs [18]. Here we will discuss and compare the earlier reported results [18] with the currently obtained data.

In the present study, the *I/V* characteristics of porcine retinal MC IFs were measured using a modified version of the earlier developed approach [16]. Once more, the *I/V* dependences were interpreted in terms of the Schottky diode theory, and the fitting parameters estimated. Our theoretical approach was based on the earlier proposed models [12,15] and the properties of the Au/IF junction, used to explain its observed behavior. The presently reported results will improve our understanding of high-contrast photopic vision of vertebrates.

2. Materials and methods

2.1. Isolation and characterization of IFs

Presently we used a modified isolation procedure based on that described earlier by Perng et al. [19]. Namely, we used freshly enucleated porcine eyes from a local slaughterhouse, originating from animals routinely slaughtered for human consumption. Therefore, the requirement for the ethics committee approval did not apply. The eyes were stored at +4 °C. We removed four retinas from these eyes, totaling 2.341 g. This material was frozen to −70 °C for 5 min and finely chopped mechanically. The homogeneously chopped material was warmed to 20 °C and mixed with 10 mL bidistilled water. 10 mg of microcrystalline diamond (Sigma-Aldrich) were added to the mixture that was ultrasonicated for 30 min at +20 °C. The mixture was then filtered using 500 nm pore diameter paper filter (Sigma Aldrich), and the liquid fraction was again filtered on a 20 nm pore diameter paper filter. The second filter was placed into a glass beaker with 10 mL of bidistilled water, and mildly ultrasonicated for 5 min at +20 °C. The suspension was centrifuged for 15 min at 25,000g on a Sorvall RC-5B, the fraction of IFs with the $150\,k \le M \le 300\,k$ apparent molecular mass was collected and used in further experiments. The selected fraction was diluted to the total volume of 10 mL and stored at + 4 °C. The total yield of the IFs was ca. 47 mg. Using the earlier proposed procedure, we estimated the IF number density [9] in the stock suspension at $3.2 \times 10^9\,cm^{-3}$. Here we assumed that the IFs were homogeneously distributed over the sample volume.

2.2. Electric conductivity measurements

The matrix of gold electrodes contained 1000 electrodes arranged in 500 electrode pairs. The matrix was produced using electron beam lithography (JBX-6300FS, JEOL), with the equivalent electrodes all connected in parallel as schematically shown in Fig. 1.

Each electrode was 1 μm wide, the distance between the electrodes in the pair was 20 nm and the distance between the two neighboring pairs was 20 μm. The total size of the matrix active area was $10 \times 20\,mm^2$, and the total electrode surface area was ca. 80% of the total electrode matrix area.

The electrode matrix was connected to the KEITHLEY 6430 source meter unit, operated by a PC computer via GPIB board (National Instruments Inc., QUANCOM PCI GPIB Card). Voltage and current were measured to better than 1%. The data acquisition system was controlled by the software running in LabView-8.0 environment, with the measurement system recording currents down to 0.1 nA.

The electrode matrix was mounted inside a Pyrex sample cell with

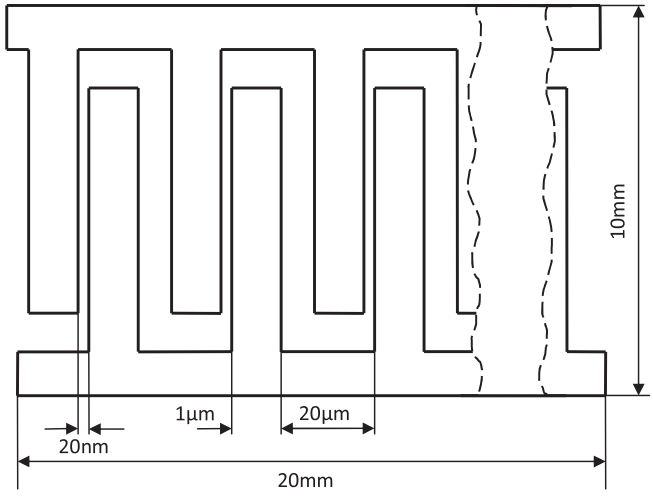

Fig. 1. Schematic drawing of the electrode matrix. The gold electrode matrix shown is $20 \times 10\,mm^2$, with 500 electrode pairs. The gap between the electrodes in the pair where the potential difference is applied is 20 nm, the electrode width is 1.0 μm, the distance between electrode pairs is 20 μm and the electrode length is 8.0 mm.

4.5 mL total volume that contained either bidistilled water or the sample suspension, and the cell was mounted into a water thermostat with temperature controllable in the 5–40 °C range. The temperature was measured to 1.0 °C, and the thermostat provided temperature control to 0.1 °C. The required number density in the measured samples was adjusted by dilution of the stock suspension with the number density $n_{IF} = 3.2 \times 10^9\,cm^{-3}$.

3. Results and discussion

Using the earlier reported information [16,17], we carried out the *I/V* measurements 800 s after filling the measurement cell with the aqueous suspension of IFs. This time interval was sufficient for the equilibrium between the IF adsorption and desorption from the matrix to be reached [16] Measurements were carried out at different temperatures in the range from 5 °C (278 K) – 40 °C (313 K) for the aqueous suspension of the MC IFs with $n_{IF} = 3.2 \times 10^8\,cm^{-3}$ obtained by diluting the stock suspension by the factor of 10. Note that previously [16] the samples with variable number density of MC IFs were used studied in different measurements, where the number density was varied in the $(0.21 \div 2.10) \times 10^8\,cm^{-3}$ range [16]. On the contrary, constant number density of $(3.2 \pm 0.1) \times 10^8\,cm^{-3}$ was used in the current measurements. The results obtained are shown in Fig. 2.

It can be seen in Fig. 2a that the negative and positive branches of the *I/V* dependence are identical. This result may be explained by the random directional distribution of the MC IFs adsorbed by the electrode matrix and relatively weak interactions of the IFs with the Au electrode surface. Taking into account this result, further on we will only discuss the positive branches in the *I/V* plots. The experimental results were fitted by the function describing the Schottky diode [12–15]:

$$I(V) = \frac{4\pi e m k_B}{h^2}\alpha(T)T^2 e^{-\frac{eU_S}{k_B T}}\left[e^{\frac{eV}{k_B T}} - 1\right] \quad (1)$$

where e is the absolute value of the electron charge, m is the effective electron mass, k_B is the Boltzmann constant, h is the Plank constant, T is the absolute temperature, I is the measured current, V is the applied voltage, U_S is the Schottky barrier, $\alpha(T)$ is the temperature-dependent function taking into account adsorption – desorption equilibrium of the IFs. Consider the adsorption – desorption equilibrium:

$$IF_{bulk} \leftrightarrow IF_{ads}$$

where IF_{bulk} and IF_{ads} are suspended IFs and adsorbed IFs, respectively.

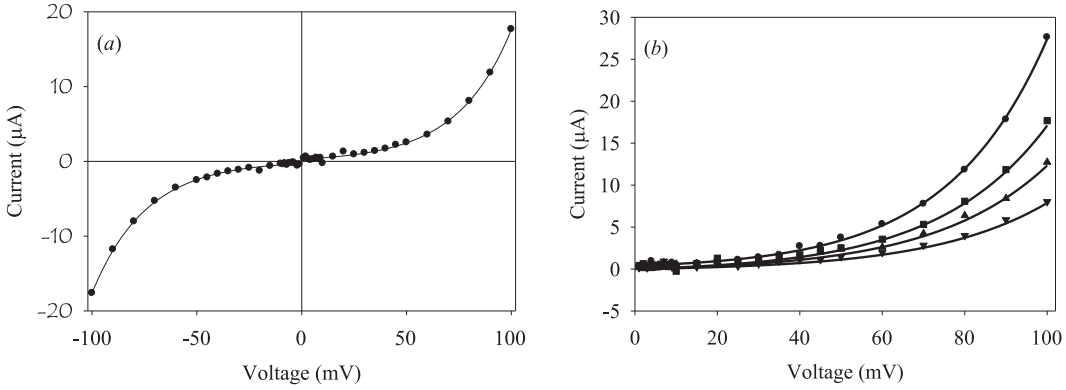

Fig. 2. (*a*) The *I/V* dependence measured at 278 K at the –100 mV to +100 mV of the external electric potential difference. (*b*) The *I/V* dependences measured in the aqueous suspension of IFs: circles – 278 K, squares – 298 K, triangles up – 308 K, and triangles down – 313 K. All measurements were carried out for the initial IF concentration $n_{IF} = 3.2 \times 10^8\ \mathrm{cm}^{-3}$.

In this case, denoting n_{ads} the number density of adsorbed IFs, and n_0 the initial number density in the suspension, we define the $\alpha(T)$ function as follows:

$$n_{ads} = \frac{e^{-\frac{\Delta G}{k_B T}} n_0}{\left(1 + e^{-\frac{\Delta G}{k_B T}}\right)} \approx e^{-\frac{\Delta G}{k_B T}} n_0 = \alpha(T) \tag{2}$$

where n_0 is the initial number density of MC IFs in the suspension, and ΔG is the Gibbs potential for the adsorption – desorption. Thus, Eq. (1) may be rewritten as follows:

$$I(V) = \frac{4\pi e m k_B}{h^2} n_0 T^2 e^{-\frac{eU_S + \Delta G}{k_B T}} \left[e^{\frac{eV}{k_B T}} - 1 \right] = A_e f T^2 e^{-\frac{eU_S + \Delta G}{k_B T}} \left[e^{\frac{eV}{k_B T}} - 1 \right]$$
$$\approx F(T) e^{S(T)V}$$
$$F(T) = \frac{4\pi e m k_B}{h^2} n_0 T^2 e^{-\frac{eU_S + \Delta G}{k_B T}}$$
$$S(T) = \frac{e}{k_B T} \tag{3}$$

The values of the fitting parameters are listed in Table 1.

The fitted temperature dependences $F(T)$ and $S(T)$ are shown in Fig. 3.

The values of the fitting parameters $Ue + \Delta G$, f and b are 7.88 ± 0.11 kcal/mol, 0.5831 ± 0.0037 and (1.154 ± 0.021) $10^4\ V^{-1}K$, respectively. Earlier we have estimated $\Delta G = -6.31$ kcal/mol [16]. Therefore, $Ue = 14.19$ kcal/mol = 0.62 eV. The slope of the linear function of Fig. 3 is about (1.15 ± 0.03) × $10^4 \approx e/k_B$. Note that the latter value is in good agreement with the ratio of the respective fundamental constants. We therefore conclude that the presently used modeling approach produces reasonable results. We also conclude that porcine MC IFs have electric properties of a semiconductor.

Note that recently [18] we reported electric field modulation of the light energy transmitted along MC IFs isolated from porcine retina. Such measurements were carried out using a different experimental design. Those experiments used a sandwich capillary matrix, with three 30 μm thick dielectric layers (Si_3N_4) interspaced by two 15 μm metal layers (Au) and 2.5 × 10^5 capillary holes each 15 nm in diameter. This capillary matrix was filled by MC IFs and their electric conductivity measured. Note that we already reported *I/V* dependence at 5 °C, which is quite well reproduced in the present report. We conclude that the two independent measurements using different approaches produced the same results, reinforcing our confidence in the correctness of the presently adopted techniques.

We should also discuss the role of Au electrodes at the Au/IF contacts. Presently we are lacking a detailed knowledge of the zone structure of the semiconducting IFs and additional experimental data obtained with other metals, that would allow to produce a detailed picture of the Au/IF interactions. However, we can compare Au/Si and Au/IF contacts, using the previously reported results on the Au/Si contacts [20]. Such contacts exhibited exponential form of the *I/V* dependence, with the Si band gap estimated from the measured curves [20]. The band gap thus estimated reproduced with acceptable accuracy the results of optical measurements. Considering Au/Si interface, the Au layer is deposited on top of the Si crystal, and diffusion of Au into Si could cause some changes in measured properties. On the other hand, strong interactions are generated at the Au/Si interface, while the effects of these interactions upon the Si bandgap are not significant. The band gap of 0.62 eV we estimated for IFs is in the near-infrared spectral range. We did not attempt to record the IF electronic absorption spectra in this range, because this range should be congested with the overtones of the IF vibrational bands. Note that all of the previously reported optical absorption bands [17,18] may be assigned to transitions between the valence and the second conductive zone of the IFs. Comparing to the Au/Si contact, the interactions at the Au/IF contact should be much weaker, as only Van der Waals forces should be present. Therefore, we do not expect any significant effects of the Au electrodes upon the electronic state structure and electronic properties of IFs in presence of the Au/IF contacts. At this time we don't have sufficient evidence that would allow discussing the mechanism of electron transport between Au and IFs. Therefore, we leave this issue for a follow-up publication.

The presently reported results demonstrate interesting properties of the natural biological fibers. These properties support and substantiate the previously hypothetic quantum mechanism of high-contrast photopic vision in vertebrate eyes [12,15]. We leave detailed quantum chemical analysis of these results for a future study.

Table 1
The values of the fitting parameters *F* and *S*.

T, K	*F*(*T*), μA	*S*(*T*), V^{-1}
278	1.02	41.7
298	2.98	38.9
308	4.85	37.7
323	9.51	35.9

4. Conclusion

In the current study, we reported the *I/V* characteristics of the MC IFs of the porcine retina. It was found that the results obtained may be interpreted as the electric behavior of the semiconducting IFs touching the gold contacts providing the electric current to these IFs. Thus, the measured dependences were fitted by the relationship (1) describing Schottky diodes. The analysis of the temperature dependence of the *I/V* experimental curves allowed to estimate the parameter values characterizing the electric conductivity of the MC IFs studied. We finally

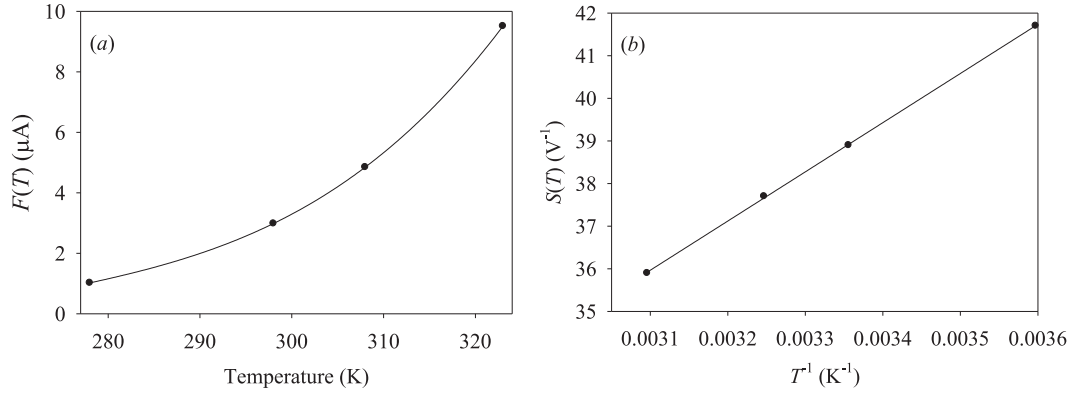

Fig. 3. Temperature dependences of (*a*) *F* and (*b*) *S* parameters, obtained by fitting the Eq. (3) to the experimental data shown in Fig. 2.

conclude that the MC intermediate filaments have the electric properties of a semiconductor with the band gap of 0.62 eV.

Acknowledgements

This project was partially supported by the Institute for Functional Nanomaterials (NSF Grant 1002410) and PR NASA EPSCoR (NASA Cooperative Agreement NNX15AK43A) grants for V. M. I. K. is grateful to Peter Stallinga for valuable discussions.

References

[1] V.I. Govardovskii, E.I. Golovanevskii, L.V. Zueva, I.I. Vasil'eva, J. Evol. Biochem. Physiol. 17 (5) (1981) 492–497.
[2] I. Solovei, M. Kreysing, Ch. Lanctot, S. Kosem, L. Peich, Th. Cremer, J. Guck, B. Joffe, Cell 137 (2009) 356–368.
[3] S. Agte, S. Junek, S. Matthias, E. Ulbricht, I. Erdmann, A. Wurm, D. Schild, J.A. Käs, A. Reichenbach, Biophys J. 101 (2011) 2611–2619, https://doi.org/10.1016/j.bpj.2011.09.062.
[4] A. Reichenbach, A. Bringmann, Müller Cells in Healthy and Diseased Retina, Springer, 2010.
[5] A. Reichenbach, A. Bringmann, New functions of Müller cells (Review), Glia 61 (2013) 651–678, https://doi.org/10.1002/glia.22477.
[6] A. Reichenbach, K. Franze, S. Agte, S. Junek, A. Wurm, J. Grosche, A. Savvinov, J. Guck, S.N. Skatchkov, Live Cells as Optical Fibers in the Vertebrate Retina, Selected Topics on Optical Fiber Technology, 73, Dr Moh. Yasin (Ed.), (2012); ISBN: 978-953-51-0091-1, InTech, Available from: https://www.intechopen.com/books/selected-topics-on-optical-fiber-technology.
[7] S. Agte, A. Savvinov, A. Karl, A. Zayas-Santiago, E. Ulbricht, V.I. Makarov, A. Reichenbach, A. Bringmann, S.N. Skatchkov, Exp. Eye Res. 173 (2018) 91–108, https://doi.org/10.1016/j.exer.2018.05.009.
[8] K. Franze, J. Grosche, S.N. Skatchkov, S. Schinkinger, C. Foja, D. Schild, U. Uckermann, K. Travis, A. Reichenbach, J. Guck, PNAS 104 (2007) 8287–8292, https://doi.org/10.1073/pnas.0611180104.
[9] A.M. Labin, S. Shadi, N.R. Erez, R. Ido, Nat. Comm. 5 (431) (2014) 1–9, https://doi.org/10.1038/ncomms5319.
[10] L. Zueva, T. Golubeva, E. Korneeva, V. Makarov, I. Khmelinskii, M. Inyushin, Microsc. Microanal. 22 (2016) 379–386, https://doi.org/10.1017/S1431927616000507.
[11] L. Zueva, V. Makarov, S.A. Zayas, T. Golubeva, E. Korneeva, A. Savinov, M. Elton, S.N. Skatchkov, M. Inyushin, J. Neurosci. Neuroeng. 3 (2014) 85–91.
[12] V. Makarov, L. Zueva, T. Golubeva, E. Korne1eva, I. Khmelinskii, M. Inyushin, 011005, J Neurophotonics 4 (2017) 1–14.
[13] I. Khmelinskii, L. Zueva, M. Inyushin, V. Makarov, Phot. Nanostruct. – Fundament. Appl. 16 (2015) 24–33.
[14] I. Khmelinskii, T. Golubeva, E. Korneeva, M. Inyushin, L. Zueva, V. Makarov, J. Photochem. Photobiol. B 173 (2017) 282–290.
[15] L. Zueva, T. Golubeva, E. Korneeva, M. Inyushin, I. Khmelinskii, V. Makarov, Archive: (2017).
[16] I. Khmelinskii, V. Makarov, Chem. Phys. J. 519 (2019) 6–20, https://doi.org/10.1016/j.chemphys.2018.11.020.
[17] I. Khmelinskii, V. Makarov, Exp. Eye Res. (2019), https://doi.org/10.1016/j.exer.2019.02.008.
[18] I. Khmelinskii, V. Makarov, Chem. Phys. Lett. (2019).
[19] M.D. Perng, L. Cairns, P. VandenIjssel, A. Prescott, A.M. Hutcheson, R.A. Quinlan, J. Cell Sci. 112 (1999) 2099–2112.
[20] H. Ayed, L. Béchir, M. Benabdesslem, N. Benslim, L. Mahdjoubi, T. Mohammed-Brahim, A. Hafdallah, M.S. Aida, J. Nano Electron. Phys. 8 (2016), https://doi.org/10.21272/jnep.8(1).01038 01938.